Crystallographic Analysis of the Human Phenylalanine Hydroxylase Catalytic Domain with Bound Catechol Inhibitors at 2.0 Å Resolution[†,‡]

Heidi Erlandsen,[§] Torgeir Flatmark,[||] Raymond C. Stevens,*[,⊥] and Edward Hough*[,§]

Protein Crystallography Group, Chemistry Department, University of Tromsø, N-9037 Tromsø, Norway, Department of Biochemistry and Molecular Biology, University of Bergen, Årstadveien 19, N-5009 Bergen, Norway, Department of Chemistry, University of California, Berkeley, California 94720, and Physical Biosciences Division at Lawrence Berkeley National Laboratory, Berkeley, California 94720

Received June 29, 1998; Revised Manuscript Received August 18, 1998

ABSTRACT: The aromatic amino acid hydroxylases represent a superfamily of structurally and functionally closely related enzymes, one of those functions being reversible inhibition by catechol derivatives. Here we present the crystal structure of the dimeric catalytic domain (residues 117−424) of human phenylalanine hydroxylase (hPheOH), cocrystallized with various potent and well-known catechol inhibitors and refined at a resolution of 2.0 Å. The catechols bind by bidentate coordination to each iron in both subunits of the dimer through the catechol hydroxyl groups, forming a blue-green colored ligand-to-metal charge-transfer complex. In addition, Glu330 and Tyr325 are identified as determinant residues in the recognition of the inhibitors. In particular, the interaction with Glu330 conforms to the structural explanation for the pH dependence of catecholamine binding to PheOH, with a pK_a value of 5.1 (20 °C). The overall structure of the catechol-bound enzyme is very similar to that of the uncomplexed enzyme (rms difference of 0.2 Å for the Cα atoms). Most striking is the replacement of two iron-bound water molecules with catechol hydroxyl groups. This change is consistent with a change in the ligand field symmetry of the high-spin ($S = 5/2$) Fe(III) from a rhombic to a nearly axial ligand field symmetry as seen upon noradrenaline binding using EPR spectroscopy [Martinez, A., Andersson, K. K., Haavik, J., and Flatmark, T. (1991) *Eur. J. Biochem. 198*, 675−682]. Crystallographic comparison with the structurally related rat tyrosine hydroxylase binary complex with the oxidized cofactor 7,8-dihydrobiopterin revealed overlapping binding sites for the catechols and the cofactor, compatible with a competitive type of inhibition of the catechols versus BH_4. The comparison demonstrates some structural differences at the active site as the potential basis for the different substrate specificity of the two enzymes.

The mononuclear non-heme iron(II) enzyme phenylalanine hydroxylase (PheOH, phenylalanine 4-monooxygenase, EC 1.14.16.1) catalyzes the hydroxylation of the essential amino acid L-phenylalanine (L-Phe)[1] to form L-tyrosine (L-Tyr) in the presence of the cofactor 6(*R*)-L-*erythro*-tetrahydrobiopterin (BH_4) and dioxygen (for reviews, see refs *1* and *2*). PheOH is structurally and functionally highly homologous to tyrosine hydroxylase (TyrOH, tyrosine 3-monooxygenase, EC 1.14.16.2) and tryptophan hydroxylase (TrpOH, tryptophan 5-monooxygenase, EC 1.14.16.4). The three enzymes have a three-domain structure with a regulatory domain, a catalytic domain, and a tetramerization domain, and they have a common structural motif for the iron active site (*3*, *4*). The motif has been referred to as a 2-His-1-carboxylate facial triad (for a review, see ref *5*). The three endogenous iron ligands are completely conserved in all known amino acid hydroxylases. The remaining coordination sites are occupied by water molecules and are accessible to exogenous ligands (*3*, *4*). The hydroxylases also share some common regulatory properties, including their activation by phosphorylation of Ser residues in the regulatory domain, and they are all inhibited by catechol binding at the active site. Importantly for TyrOH, the enzyme is subject to feedback inhibition by dopamine, noradrenaline, and adrenaline (Scheme 1), which is considered to be physiologically significant in catecholaminergic neuroendocrine cells (*2*, *6*, *7*). The catecholamines coordinate to the iron center with a relatively high affinity [$IC_{50} \approx 2$ μM for TyrOH (*8*)], giving rise to ligand-to-metal charge-transfer (LMCT) bands with an absorbance maximum at 695−700 nm yielding a blue-green colored protein (*9*). Similar charge-transfer complexes are

[†] This work was supported by grants from the Research Council of Norway (H.E., E.H., and T.F.), Rebergs legat (T.F.), the Novo Nordisk Foundation (T.F.), the European Comission (T.F.), and the Physical Biosciences Division of Lawrence Berkeley National Laboratories (R.C.S.).

[‡] The coordinates have been deposited with the Brookhaven Protein Data Bank (PDB), with accession numbers 3PAH, 4PAH, 5PAH, and 6PAH for the adrenaline, noradrenaline, dopamine, and L-DOPA complexes, respectively.

* To whom correspondence should be addressed. E-mail for R.C.S.: stevens@adrenaline.berkeley.edu. E-mail for E.H.: edward.hough@chem.uit.no.

[§] University of Tromsø.

[||] University of Bergen.

[⊥] University of California and Physical Biosciences Division at Lawrence Berkeley National Laboratory.

[1] Abbreviations: hPheOH, human phenylalanine hydroxylase; L-Phe, L-phenylalanine; L-Tyr, L-tyrosine; BH_4, 6(*R*)-L-*erythro*-tetrahydrobiopterin; BH_2, 7,8-dihydrobiopterin; TyrOH, tyrosine hydroxylase; TrpOH, tryptophan hydroxylase; L-DOPA, L-dihydroxyphenylalanine; ^{1}H NMR, proton nuclear magnetic resonance; EPR, electron paramagnetic resonance; LMCT, ligand-to-metal charge-transfer.

10.1021/bi9815290 CCC: $15.00
Published on Web 10/21/1998

Scheme 1

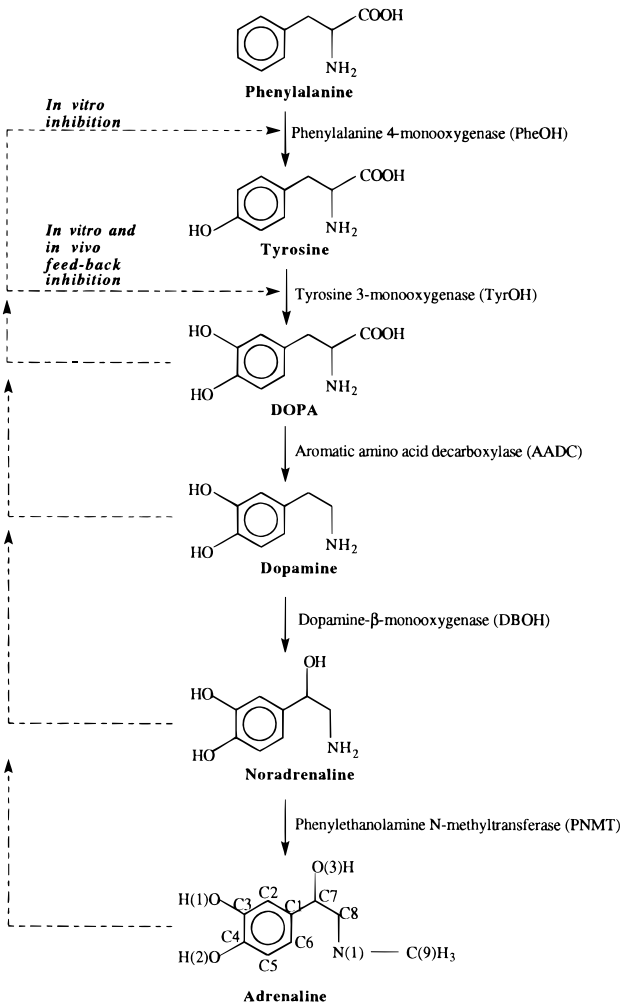

formed between catecholamines and PheOH (*10*). The TyrOH enzyme activity is inhibited by catechols competitively with respect to the tetrahydrobiopterin cofactor and noncompetitively with respect to L-Phe and/or L-Tyr (8). For both PheOH and TyrOH, the iron atom and a charged amino acid lining the crevice structure of the active site have been considered to be involved in the binding of the catecholamines (*10*, *11*). Protonation of the charged group near the active site, with an apparent pK_a of 5.3 for TyrOH (*11*) and 5.1 for PheOH (*10*), increases the rate constant for the dissociation (off-rate) of catecholamines more than 100-fold in TyrOH (*11*).

The crystal structures of the C-terminal domain of both TyrOH (*3*) and PheOH (*4*, *12*) (corresponding to the catalytic and the tetramerization domains) have recently been determined. The overall three-dimensional structures of the corresponding catalytic domains have been found to be very similar. Both structures contain a ferric iron, with two His (PheOH, 285 and 290; TyrOH, 331 and 336) and one Glu (PheOH, 330; TyrOH, 376) as ligands coordinating to the ferric iron. The active site is solvent exposed in both enzyme forms, and the iron is six-coordinate in PheOH with the remaining nonprotein coordination sites occupied by water molecules (*4*). To investigate the mechanism of catecholamine inhibition, crystallographic studies were conducted on dopamine−, noradrenaline−, adrenaline−, and L-dihydroxyphenylalanine (L-DOPA)−PheOH complexes. Given the fact that the catechol inhibition and interaction with the active site are very similar in the two hydroxylases as seen by spectroscopic methods (*2*), the information obtained is relevant for the proposed physiologically important feedback inhibition of TyrOH in catecholaminergic neuroendocrine cells.

MATERIALS AND METHODS

Data Collection and Processing. Recombinant hPheOH was expressed and purified as previously described (*13*, *14*). The inhibitor complexes were prepared by preincubating the enzyme with 1 mM catechol (about 5-fold excess with

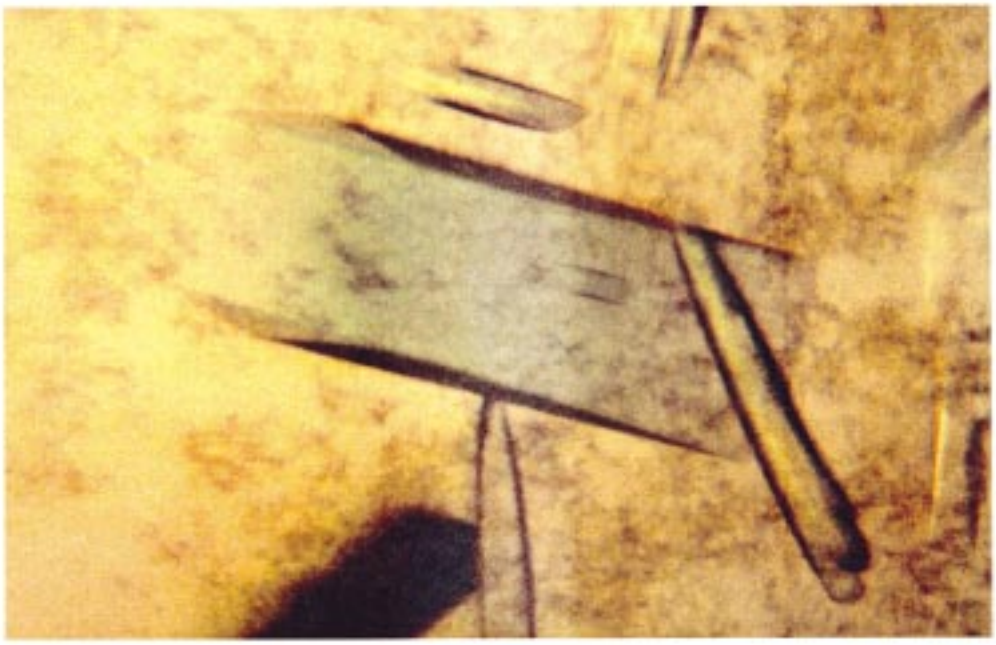

FIGURE 1: Crystals of the catecholamine complexed with PheOH. The blue-green color of the crystal is due to the catechol complexed with the ferric iron. The picture was taken with nonpolarized light to ensure that the natural blue-green color of the crystal was seen correctly.

Table 1: Data Collection, Processing, and Refinement Statistics

	L-DOPA	dopamine	noradrenaline	adrenaline
SSRL beamline used	9-1	9-1	7-1	7-1
no. of crystals	4	4	1	1
space group	*C*2221	*C*2221	*C*2221	*C*2221
unit cell parameters (Å)	$a = 66.89$, $b = 109.12$, $c = 125.71$	$a = 66.84$, $b = 109.17$, $c = 125.80$	$a = 66.78$, $b = 108.73$, $c = 125.46$	$a = 66.70$, $b = 108.65$, $c = 125.47$
resolution range (Å)	20−2.15 (2.23−2.15)	20−2.10 (2.17−2.10)	50−2.0 (2.07−2.00)	50−2.0 (2.07−2.00)
no. of reflections	25115	26720	30846	30303
redundancy	5−6	5−6	5−6	4
completeness (Å)	98.8 (99.3)	98.5 (99.8)	98.8 (98.3)	96.4 (93.8)
$R_{sym}(I)$ (%)	6.8 (30.7)	6.1 (26.7)	5.1 (24.6)	5.1 (33.0)
no. of reflections used in refinement ($F > 2\sigma F$)	22763	24638	30512	29656
resolution range (Å)	20−2.15	20−2.1	20.0−2.0	20.0−2.0
R_{cryst} (%)	17.1	16.4	16.3	17.6
R_{free} (%)	20.3	20.0	20.4	20.7
no. of structural waters	114	129	126	107
estimated coordinate error from Luzatti plot (Å)	0.20	0.18	0.18	0.19
rms deviation for bond lengths (Å)	0.018	0.018	0.019	0.018
rms deviation for bond angles (deg)	1.8	1.8	1.9	1.8
rms deviation for dihedral angles (deg)	21.7	21.3	21.5	21.4
rms deviation for improper angles (deg)	1.10	1.12	1.14	1.09
overall *B*-value (Å^2)	25.7	28.3	25.2	26.0
mean *B* for catechol (Å^2)	54.8	48.0	41.9	36.5

respect to the protein concentration), before setting up cocrystallization experiments. The crystals grew to the same size and under the same conditions [10−16% PEG 2000, 0.05−0.08 M PIPES buffer (pH 6.8), and 6−12 mg/mL protein] as those of the native truncated form of PheOH (consisting of residues 103−427) (*14*).

Synchrotron data were collected at the Stanford Synchrotron Radiation Laboratory (SSRL), beamline 7-1 (noradrenaline and adrenaline complexes) and beamline 9-1 (dopamine and L-DOPA complexes), using 1.08 (7-1) and 0.98 Å wavelength radiation (9-1), respectively. The data were collected at 4 °C on one to four crystals of each complex and by translating the crystals several times to expose new parts when the crystal started to lose diffraction intensity. The crystals were mounted in glass capillaries and kept on ice until they were put in the X-ray beam. The data were collected on a MAR detector (MAR Research). The crystals were isomorphous with the native crystals in space group $C222_1$. Data processing was performed using the programs DENZO and SCALEPACK (*15*). The data collection and processing statistics are presented in Table 1 for each of the inhibitor complexes.

Structure Solution and Refinement. The positions of the catechol molecules were determined by calculating a difference electron density map ($F_{obs} - F_{calc}$), using the native structure as a model for the calculated phases. Density for the catechol moiety of the catecholamines could clearly be seen at a contour level of up to 2.5σ for the adrenaline and noradrenaline data sets, even before any refinement was initiated. The catechol L-DOPA and catecholamine dopamine could be seen at a contour level of 1.5σ. All refinement of the structures and composite omit map calculations (*16*) were performed with the program CNS (version 0.3) (*17*). Ten percent of the data were set off for cross validation of refinement (the R_{free} value; *18*). The program O (*19*) was used to manually fit the differences from the native structure into the experimental density, using composite σ-weighted $2F_{obs} - F_{calc}$ and $F_{obs} - F_{calc}$ omit maps, with spheres of 8−10% of the atoms omitted from the model. The refinement statistics are presented in Table 1 for each of the inhibitor complexes.

Table 2: Atomic Distances between Important Active Site Residues in the PheOH−Catechol Complexes

	L-DOPA	dopamine	noradrenaline	adrenaline
catechol O1−Fe(III) (Å)	2.0	2.0	2.0	2.1
catechol O2−Fe(III) (Å)	2.1	2.0	2.0	2.1
His285 Nϵ2−Fe(III) (Å)	2.2	2.2	2.1	2.1
His290 Nϵ2−Fe(III) (Å)	2.2	2.1	2.0	2.2
Glu330 Oϵ2−Fe(III) (Å)	2.0	1.9	1.9	1.9
Wat−Fe(III) (Å)	2.4	2.3	2.3	2.3
Tyr325 OH−catechol O2 (Å)	2.7	2.9	2.6	2.6
Glu330 Oϵ2−catechol O2 (Å)	2.6	2.7	2.6	2.5
Wat−catechol O1 (Å)	3.1	3.0	3.0	3.0
Glu286 Oϵ2−Wat (Å)	2.5	2.6	2.6	2.6

RESULTS

The crystallization of the catecholamine complexes of PheOH produced blue-green crystals (Figure 1), indicating that a complex between ferric iron and catechol was formed (*9*, *20*). The position of the dopamine, noradrenaline, and adrenaline molecules could easily be determined from the difference maps. The density for the L-DOPA molecule was not as good as that for the catecholamines, but could be seen in the same position as the other inhibitors, and was therefore interpreted as the catechol moiety of the L-DOPA molecule.

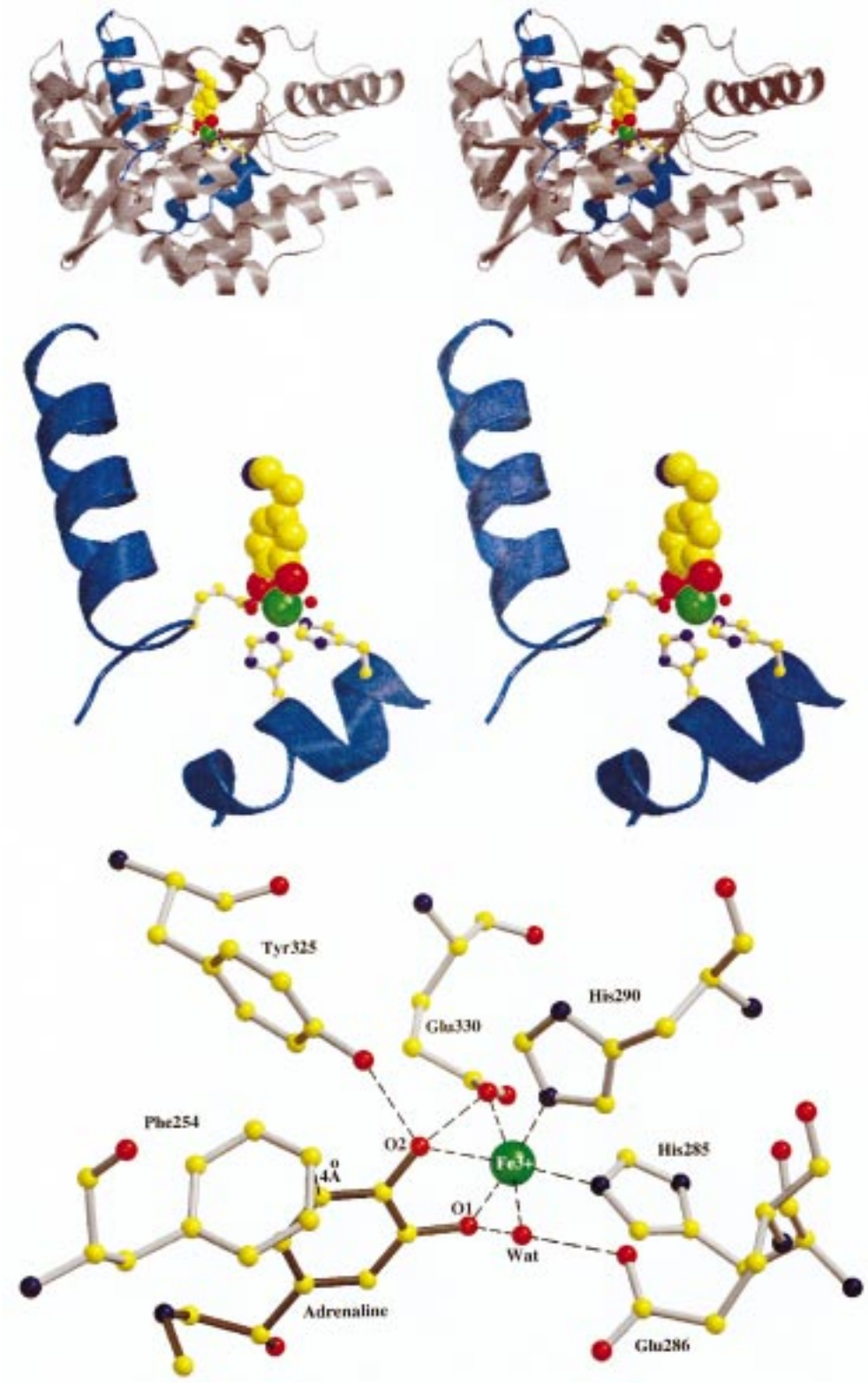

FIGURE 2: (A, top) Overview of the PheOH monomer with the catecholamine inhibitor adrenaline shown as a cpk model in the active site together with the coordinating residues (His285, His290, and Glu330) and a water molecule. The region between residues 284−295 and 315−333 is blue, and the rest of the molecule is gray. For the cpk model, the iron is green, the oxygen atoms are red, the nitrogen atoms are blue, and the carbon atoms are yellow. (B, middle) Closeup of the region involved in iron coordination shown in blue in panel A. (C, bottom) Important active site residues in the catechol−PheOH complexes are shown for the PheOH−adrenaline complex. Distances between the same residues for all four complexes are presented in Table 2. The catechol molecule is dark gray, and the ferric iron is green. The figures were produced with the programs Molscript (*35*) and Raster3D (*36*).

The crystals of the L-DOPA complex also had the blue-green color, indicating that the same complex between ferric iron and catechol was formed. Figure 2 displays the binding site of the catechols in PheOH. The hydroxyl groups of the catechol are directly coordinated to the ferric iron with an O1−Fe distance of 2.0−2.1 Å and an O2−Fe distance of

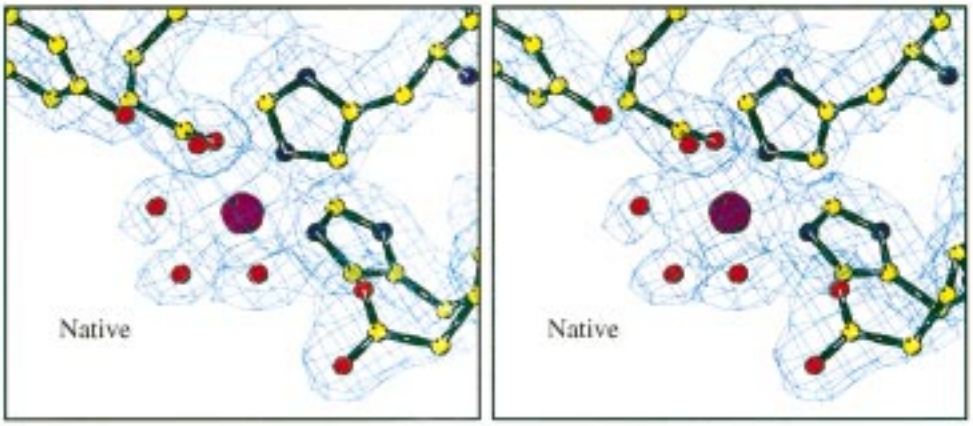

FIGURE 3: (A, top panel) Stereoview of the $2F_{obs} - F_{calc}$ σ-weighted electron density for the active site residues in the native, iron-only, PheOH structure (*4*). The resolution range used in the map calculation is 20−2.0 Å, and the contour level is 1.7σ. (B−E, facing page, four panels) Stereoviews of the $2F_{obs} - F_{calc}$ σ-weighted electron density for the PheOH−catechol complexes with adrenaline, noradrenaline, dopamine, and L-DOPA, respectively. The catechols were omitted from the map calculations in panels B−E. The resolution ranges for the catechol−PheOH complexes used in the map calculations are the same as the ones listed in Table 1, and the contour level is 1.3σ. The same residues in the active site that are shown in Figure 2C are shown, except for Phe254, which was omitted for clarity. The maps were calculated with the program CNS (*17*). The figures were produced with the program Bobscript (*37*).

2.0−2.1 Å. The same protein ligands as in the native structure are coordinated to the iron, His285 (Fe−Nϵ2 distance of 2.1 Å), His290 (Fe−Nϵ2 distance of 2.1 Å), and Glu330 (Fe−Oϵ2 distance of 1.9 Å), as well as one water molecule (opposite Glu330) (Fe−OH2 distance of 2.3 Å). The catechol hydroxyl groups bind to the iron atom with bidentate coordination, occupying one axial and one equatorial position. One of the catechol hydroxyl groups interacts with the side chain hydroxyl of Tyr325 (O2−OH distance of 2.6−2.9 Å) and also with the side chain oxygen of Glu330 (O2−Oϵ2 distance of 2.5−2.7 Å). The distances in all four complexes are presented in Table 2 and depicted in Figure 2C for the adrenaline complex.

The amino ends of the catechol molecules are solvent exposed and are not completely defined in electron density, as seen in Figure 3. The catecholamine molecule could be rotated 180° (on an axis between the catechol oxygens) between separate rounds of rebuilding and refinement without any change in the agreement statistics or unfavorable collisions with protein atoms. On the basis of the shape of the electron density surrounding the catecholamines, it appears that the molecules can bind in two different conformations, differing only in the 180° rotation around the imaginary axis through the catechols oxygens, and thus resulting in a disorder in the remaining amino end of the catechols.

The final model of the complexes includes 308 protein residues (117−424), one ferric iron, the catechol molecule, and 107−126 water molecules. The final refinement statistics are presented in Table 1 for each complex.

DISCUSSION

The mononuclear non-heme iron-containing enzyme PheOH catalyzes the hydroxylation of L-Phe to L-Tyr using BH_4 as the electron donor to reduce the iron to its catalytically active form (*21*) and dioxygen to the peroxide oxidation state (*22, 23*). Although recent crystallographic studies on recombinant human PheOH (*4*, *12*) have defined its active site structure and the nature of the iron coordination sphere, the catalytic mechanism is still a matter of discussion (for reviews, see refs *2* and *5*). Furthermore, despite having the crystal structure of both PheOH and TyrOH (*3*), we still do not understand how the amino acid side chains lining the crevice structure, notably those around the iron center, contribute to the substrate binding specificity and catalytic reaction. In contrast to other mononuclear non-heme iron(II) enzymes (*5*), there is no evidence that the substrates coordinate directly to the iron center of TyrOH (*24*, *25*) and PheOH (*26*). ^{1}H NMR spectroscopic studies have clearly demonstrated that both L-Phe (*24*) and BH_4 (*25*) bind, as binary enzyme−substrate complexes, in close proximity to the active site iron of TyrOH, but in the "second coordination sphere" of the metal. Kinetic studies suggest that BH_4 binds to TyrOH first followed by O_2 and finally tyrosine (*27*). In contrast to the substrates, the catecholamine inhibitors coordinate directly to the metal center, forming blue-green LMCT complexes as first described for TyrOH (*9*).

The molecular basis for the observed competitive type of inhibition by catecholamines (vs the pterin cofactor) of the PheOH- and TyrOH-catalyzed hydroxylations was investigated in this study using X-ray crystallography of the L-DOPA, dopamine, noradrenaline, and adrenaline binary complexes of a dimeric (and activated) truncated form (residues 117−424, "catalytic domain") of PheOH. The blue-green catecholamine−protein complexes crystallized with the same space group ($C222_1$) as the ligand-free enzyme form (*4*, *14*) and revealed LMCT bands similar to those reported for the full-length enzyme (Figure 1 and data not shown). Furthermore, the same high crystallographic resolution (2.0−2.1 Å) was obtained for all the catechol complexes that was recently reported for the ligand-free enzyme form (*4*). The electron density of the catechol moiety clearly shows that the inhibitors bind to the iron center by a bidentate coordination of the two hydroxyl groups (distances of 2.0−2.1 Å), in agreement with the interpretation of the light absorption and resonance Raman spectroscopic data (*9*, *28*). The same 2-His-1-carboxylate motif bound to the active site iron was observed in both the inhibitor and unbound forms

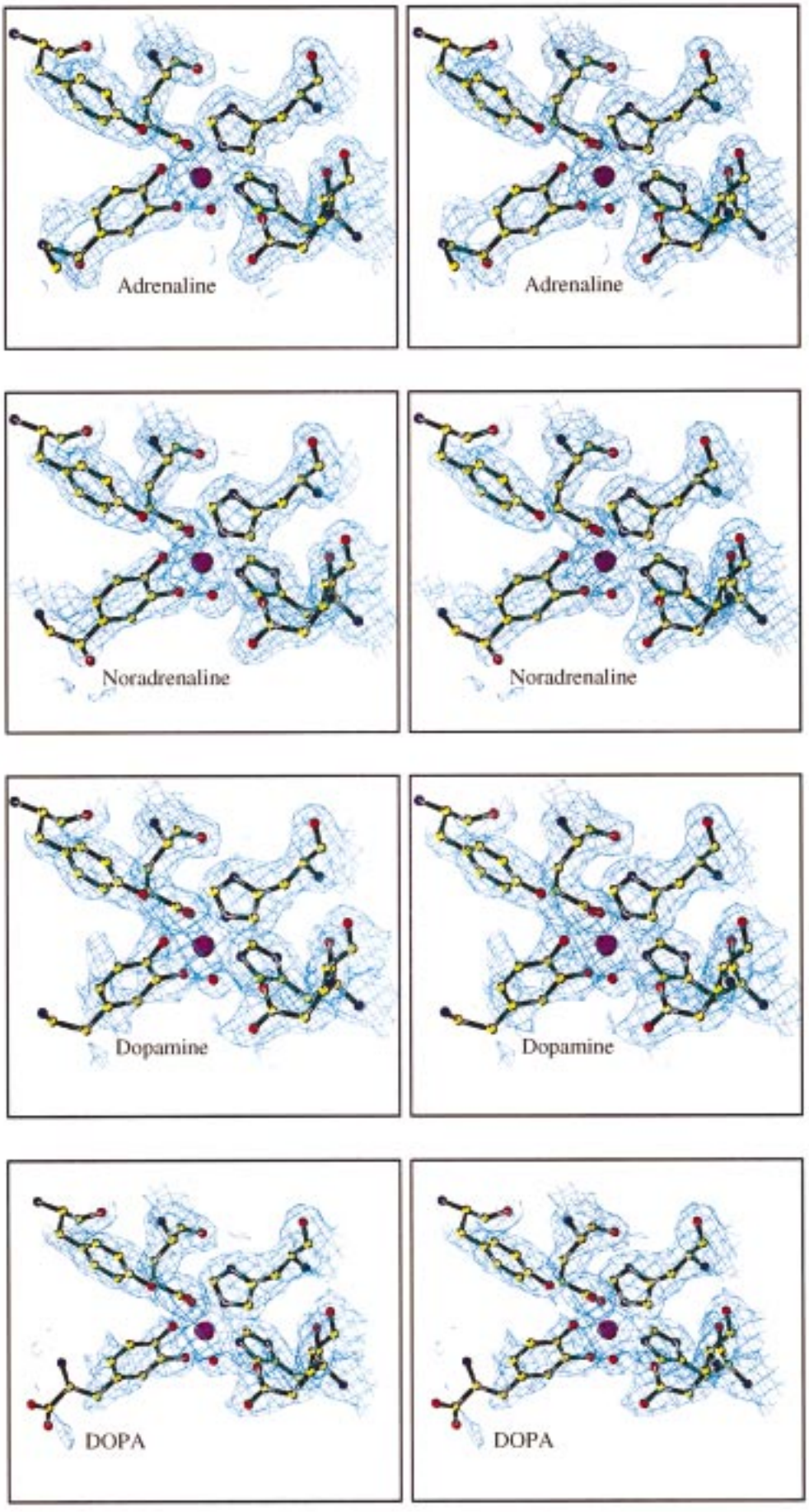
Adrenaline
Adrenaline
Noradrenaline
Noradrenaline
Dopamine
Dopamine
DOPA
DOPA

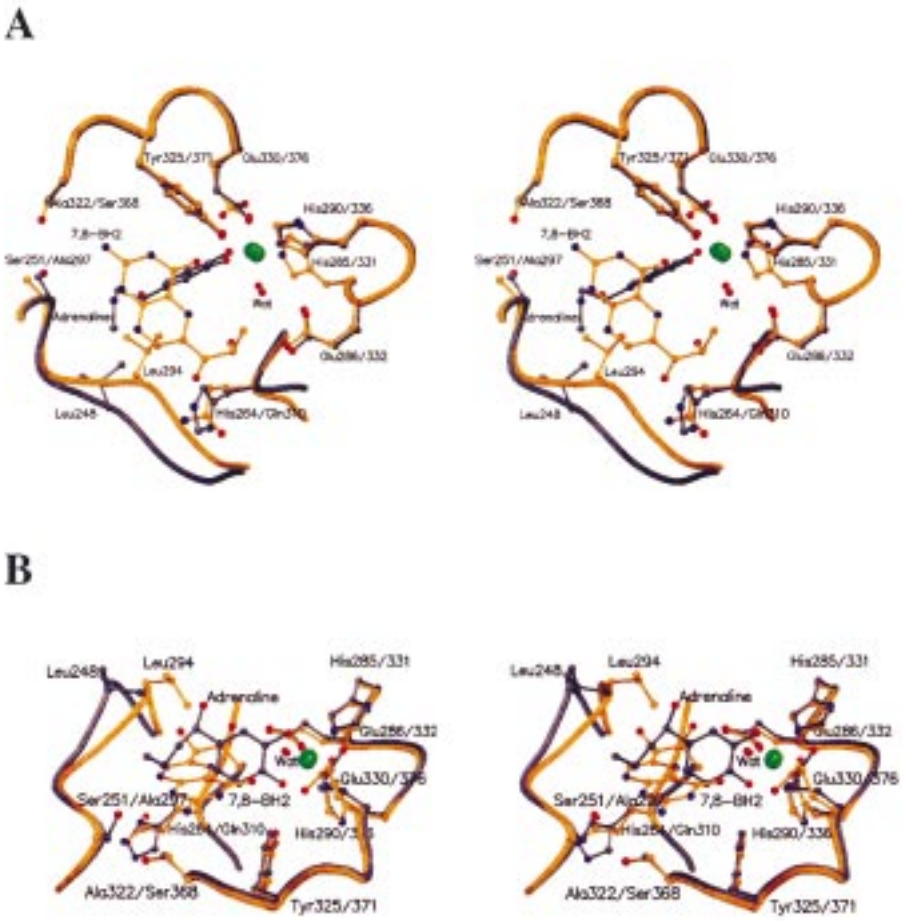

FIGURE 4: (A) Stereoview of the active site of the PheOH−adrenaline complex (gray) superimposed on the TyrOH−7,8-dihydrobiopterin complex (orange). The region of superimposition was chosen to be the Cα atoms of residues 281−319 (PheOH) and 327−365 (TyrOH) because this gave the best rms fit (0.34 Å). The individual oxygen atoms are red, the nitrogen atoms blue, and the iron atoms green. (B) Structure depicted in panel A but with another orientation. The figures were produced with the programs Molscript (*35*) and Raster3D (*36*).

of the enzyme, along with one liganded water molecule for the inhibitor complexes. The four catecholamine−PheOH complexes are structurally identical, with no significant conformational differences (rmsd of 0.08−0.18 Å), well within estimated coordinate error (residues 117−424 used in the superimposition calculations). Only a slightly larger difference was observed when these structures were compared with the ligand-free native structure, where the catecholamine−PheOH complexes superimpose on the native structure with a rms displacement of 0.19−0.22 Å, implying very minor conformational changes on ligand binding. The replacement of two water molecules with the catechol hydroxyl groups is compatible with a change in the ligand field symmetry of the high-spin ($S = {}^5/_2$) Fe(III) from a rhombic (signal at $g = 4.3$) to a nearly axial ligand field symmetry (signals at $g = 7.0$, 5.2, and 1.9) on noradrenaline binding, as seen by EPR spectroscopy (*29*).

In addition to the bidentate coordination to the iron center, the catecholamines hydrogen bond with Glu330 and Tyr325 at the active site (distances of 2.6 Å between both O2 and Tyr325 OH and Glu330 Oε2). These two residues may be involved in the stabilization of the relatively high-affinity binding ($S_{0.5} < 1$ μM) of the amines at neutral pH (*10*). Both residues are highly conserved in the aromatic amino acid hydroxylases (*3*). Thus, according to the measured pH dependence for the dissociation of L-[^{3}H]noradrenaline from the hydroxylases, a group with an apparent pK_a of 5.1 (at 20 °C) in rat PheOH and a pK_a of 5.3 (at 4 °C) in bovine TyrOH has been found to be involved in the tight binding of the inhibitor at neutral pH (*10*, *11*). The closest protein residue to the catecholamine molecule that could satisfy the apparent pK_a value is Glu330. Protonation of Glu330 in PheOH at a lower pH could reverse the stabilizing effect that its carboxyl group has on the proton of the catechol hydroxyl group.

Natural catecholamines such as dopamine, noradrenaline, and adrenaline are potent inhibitors of TyrOH (*9*) and PheOH (*10*) due to their tight binding to Fe(III) at the active site of the enzymes. ^{1}H NMR and EPR spectroscopy has shown that the addition of stoichiometric amounts of dopamine to human TyrOH−Fe(II) results in an oxidation of the iron to Fe(III) and the formation of the characteristic catechol-to-iron charge-transfer complex (*30*). This complex represents a reversibly inactive form of the enzyme in which the reduction of its ferric state by BH_4, and thereby generation of a catalytically competent form [Fe(II) oxidation level] of the enzyme, is prevented (*21*). The same binding mode has been proposed for the catechol L-DOPA, the product of the TyrOH reaction, but the fact that its binding affinity is lower than that of the catecholamines may be due to its electrostati-

cally less favorable carboxyl side chain (*8*). However, the PheOH−DOPA complex does not show any significant positional difference with respect to the other PheOH−catecholamine complexes.

The crystal structure of the binary complex of the tetrameric (and activated) truncated form (residues 164−498) of rat TyrOH with the oxidized pterin cofactor [7,8-dihydrobiopterin (BH_2)] (*31*) demonstrates that the cofactor and the catecholamines overlap when they bind at the active site (Figure 4), as can be expected from the competitive type of inhibition of the respective enzyme activities by the catecholamines. Superimposition of TyrOH and PheOH active site residues [Pro281−Glu319 (PheOH) and Pro327−Glu365 (TyrOH)], with bound cofactor and adrenaline, respectively, revealed a number of intriguing observations. The carbonyl oxygen in the C4 position on the pterin ring, as well as the C4a and C4 atoms, overlaps with the C5 and C6 atoms on the catecholamine inhibitor in the PheOH structure (atom numbering on adrenaline molecule in Scheme 1). Most of the active site residues are conserved in rat TyrOH and human PheOH. The loop of residues 245−250 in PheOH (residues 291−296 in TyrOH) exhibits the largest positional differences. In the TyrOH−pterin structure, this region is involved in binding the pterin cofactor. Specifically, hydrogen bonds are observed between the enzyme main chain carbonyl oxygen and the N8 of BH_2. This loop packs close to another region (hPheOH residues 128−141) in which all 12 residues are different in comparison to rat TyrOH. In rat TyrOH, no electron density was observed for this region of the structure (residues 176−187) (*3*). Another important residue difference between the two hydroxylases is Gln310 in TyrOH which hydrogen bonds by its carbonyl oxygen to the C2′ hydroxyl group on the dihydroxypropyl chain on BH_2, and is also stabilized by hydrogen bonds to Ser303 Oγ. In hPheOH, this residue is replaced by His264, which hydrogen bonds through one water molecule on each side to the carbonyl oxygens of residues Phe254 and Leu128. Two other amino acid differences in the active site are residues Ser251 in hPheOH (Ala297 in rat TyrOH) and Ala322 in hPheOH (Ser368 in rat TyrOH). Both these residues are between 3.7 and 3.9 Å away from the C2 amine in the pterin and about 2.8 Å away from each other. Other than the above observations, there do not seem to be any obvious differences between the active site residues in PheOH and TyrOH that can easily explain the differences in substrate specificity between the enzymes. Although the crystallization of the binary complex of L-Phe and hPheOH has been unsuccessful so far, ^{1}H NMR studies on the full-length rat (*29*) and human (*32*) enzyme have revealed that the binding site of L-Phe partially overlaps the binding site of noradrenaline. Future crystallographic studies on binary complexes between PheOH and TyrOH with their respective L-Phe and L-Tyr substrates should contribute to a better understanding of the mode of substrate binding, and possibly the mechanism of hydroxylation.

The poorly defined density of the amino part of the catecholamines in the PheOH complexes and the lack of protein interactions made by this part of the catecholamines suggest that the catechol can bind in two equivalent positions, with the plane of the catechol ring rotated 180° around an axis passing between the two hydroxyl groups of the catechol moiety. The solvent-exposed active site (see Figure 2) is consistent with the report that both (*R*)- and (*S*)-adrenaline are equally effective in their inhibition of PheOH (*33*). Therefore, the interactions contributing to the strong binding of these inhibitors would occur mainly on the basis of the LMCT interactions between the hydroxyl groups of the catecholamines and the iron (*34*). The strongest requirement that seems to be important to inhibition is an intact catechol moiety (1,2-benzenediol) (*8*). The amino moiety is less important, though in the case of L-DOPA inhibition, the measured 10-fold lower binding affinity for the TyrOH−DOPA complex (*8*) may be due to its electrostatically less favorable carboxyl side chain. The crystal structures of the inhibitor complexes show that the binding occurs predominantly by the catechol moiety with LMCT interactions to the iron and through hydrogen bonds to Tyr325 and Glu330, producing a pH-dependent release of the catechol inhibitors.

ACKNOWLEDGMENT

We thank Albert E. Beuscher, Dr. Kenneth E. Goodwill, and Prof. Aurora Martínez for valuable discussions and suggestions in preparing the manuscript. Dr. Per M. Knappskog is thanked for providing the bacterial strains expressing the truncated dimeric PheOH, and Randi M. Svebak and Ali S. Muñoz are also thanked for their expert technical assistance in preparing large amounts of pure protein for crystallization.

REFERENCES

1. Kaufman, S. (1995) *Adv. Enzymol. 70*, 103−220.
2. Kappock, T. J., and Caradonna, J. P. (1996) *Chem. Rev. 96*, 2659−2756.
3. Goodwill, K. E., Sabatier, C., Marks, C., Raag, R., Fitzpatrick, P. F., and Stevens, R. C. (1997) *Nat. Struct. Biol. 4*, 578−585.
4. Erlandsen, H., Fusetti, F., Martinez, A., Hough, E., Flatmark, T., and Stevens, R. C. (1997) *Nat. Struct. Biol. 4*, 995−1000.
5. Hegg, E. L., and Que, L. (1997) *Eur. J. Biochem. 250*, 625−629.
6. Perlman, R. L., and Sheard, B. E. (1982) *Biochim. Biophys. Acta 719*, 334−340.
7. Haavik, J., Døskeland, A. P., and Flatmark, T. (1986) *Eur. J. Biochem. 160*, 1−8.
8. Almås, B., Le Bourdelles, B., Flatmark, T., Mallet, J., and Haavik, J. (1992*) Eur. J. Biochem. 209*, 249−255.
9. Andersson, K. K., Cox, D. D., Que, L., Jr., Flatmark, T., and Haavik, J. (1988) *J. Biol. Chem. 263*, 18621−18626.
10. Martinez, A., Haavik, J., and Flatmark, T. (1990) *Eur. J. Biochem. 193*, 211−219.
11. Haavik, J., Martinez, A., and Flatmark, T. (1990) *FEBS Lett. 262*, 363−365.
12. Fusetti, F., Erlandsen, H., Flatmark, T., and Stevens, R. C. (1998) *J. Biol. Chem. 273*, 16962−16967.
13. Martinez, A., Knappskog, P. M., Olafsdottir, S., Døskeland, A. P., Eiken, H. G., Svebak, R. M., Bozzini, M., Apold, J., and Flatmark, T. (1995) *Biochem. J. 306*, 589−597.
14. Erlandsen, H., Martinez, A., Knappskog, P. M., Haavik, J., Hough, E., and Flatmark, T. (1997) *FEBS Lett. 406*, 171−174.
15. Otwinowski, Z. (1993) in *Data Collection and Processing* (Sawyer, L., Isaacs, N., and Bailey, S., Eds.) Science and Engineering Research Council, Warrington, U.K.
16. Hodel, A., Kim, S.-H., and Brunger, A. T (1992) *Acta Crystallogr. A48*, 851−858.
17. Brünger, A. T., Adams, P. D., Clore, G. M., DeLano, W. L., Gross, P., Grosse-Kunstleve, R. W., Jiang, J.-S., Kuszewski, J., Nilges, M., Pannu, N. S., Read, R. J., Rice, L. M., Simonson, T., and Warren, G. L. (1998) *Acta Crystallogr. D54*, 905−921.
18. Brunger, A. T. (1992) *Nature 355*, 472−475.

19. Jones, T. A., Zou, J.-Y., Cowan, S. W., and Kjeldgaard, M. (1991) *Acta Crystallogr. A47*, 110−119.
20. Cox, D. D., Benkovic, S. J., Bloom, L. M., Bradley, F. C., Nelson, M. J., Que, L., Jr., and Wallick, D. E. (1988) *J. Am. Chem. Soc. 110*, 2026−2032.
21. Marota, J. J. A., and Shiman, R. (1984) *Biochemistry 23*, 1303−1311.
22. Dix, T. A., and Benkovic, S. J. (1985) *Biochemistry 24*, 5839−5846.
23. Dix, T. A., Bollag, G. E., Domanico, P. L., and Benkovic, S. J. (1985) *Biochemistry 24*, 2955−2958.
24. Martinez, A., Olafsdottir, S., and Flatmark, T. (1993) *Eur. J. Biochem. 211*, 259−266.
25. Martinez, A., Vageli, O., Pfleiderer, W., and Flatmark, T. (1998) *Pteridines 9*, 44−52.
26. Loeb, K. E., Westre, T. E., Kappock, T. J., Mitic, N., Glasfeld, E., Caradonna, J. P., Hedman, B., Hodgson, K. O., and Solomon, E. I. (1997) *J. Am. Chem. Soc. 119*, 1901−1915.
27. Fitzpatrick, P. F. (1991) *Biochemistry 30*, 3658−3662.
28. Michaud-Soret, I., Andersson, K. K., Que, L., Jr., and Haavik, J. (1995) *Biochemistry 34*, 5504−5510.
29. Martinez, A., Andersson, K., Haavik, J., and Flatmark, T. (1991) *Eur. J. Biochem. 198*, 675−682.
30. Haavik, J., Martinez, A., Olafsdottir, S., Mallet, J., and Flatmark, T. (1992) *Eur. J. Biochem. 210*, 23−31.
31. Goodwill, K. E., Sabatier, C., and Stevens, R. C. (1998) *Biochemistry 37*, 13437−13445.
32. Teigen, K., Frøystein, N. Å., and Martinez, A. (1998) *Abstract Communication from the Fourth European Biological Inorganic Chemistry Conference*, p 179.
33. Miller, M., and Shiman, R. (1976) *J. Biol. Chem. 251*, 3671−3676.
34. Shiman, R. (1985) in *Folates and Pterins, Volume 2, Chemistry and Biochemistry of Pterins* (Blakeley, R. L., and Benkovic, S. J., Eds.) John Wiley & Sons, New York.
35. Kraulis, P. J. (1991) *J. Appl. Crystallogr. 24*, 946−950.
36. Merritt, E. A., and Bacon, D. J. (1997) *Methods Enzymol. 277*, 505−524.
37. Esnouf, R. M. (1997) *J. Mol. Graphics 15*, 132−134.

BI9815290